Dept. of Mech. Eng.
CUET

Published Online March 2015 (http://www.cuet.ac.bd/merj/index.html)

Mechanical Engineering Research Journal

Vol. 9, pp. 79–85, 2013

ISSN: 1990-5491

THERMAL ANALYSES OF NANO- AND MICRO- SATELLITES POINTING TO THE EARTH WITH DEPLOYABLE SOLAR PANEL ON SUN-SYNCHRONOUS ORBIT BY SMALL NUMBER OF NODES

T. K. Das[1*], T. Totani[2], M. Wakita[2] and H. Nagata[2]

[1]Graduate school of Engineering, Hokkaido University, Japan
[2]Faculty of Engineering, Hokkaido University, Japan

Abstract: This paper represents thermal analysis of nano and micro satellites of 50 kg mass and 50 cm cube pointing to the Earth with 2 kg mass and 50 cm square length deployable solar panel (DSP) in sun-synchronous and circular orbits at altitude of 500 km using few nodal analyses. So many satellites of smaller size, nano and micro satellites such as STARS, RISESAT are launched for Earth observation mission. This paper compares the projected area of satellite with and without DSP at local time of descending node (LTDN) 10 in order to explain the comparative advantages of satellite with DSP over satellite without DSP. In addition, power generation of satellite with DSP is calculated from LTDN 6 to 12 considering the solar cells are mounted completely on 5 surfaces of the main part of the satellite (MPS) and topsides of DSP that means no solar cells on earth pointing surface of the satellite and the bottom sides of DSP. The highest average power generation is obtained 149.47 W and 132.65 W at LTDN 11 in the worst hot case and the worst cold case respectively. Finally, Numbers of combinations of optical properties of micro and nano satellites with DSP for all LTDN are carried out which is higher in the case of LTDN without shadow region than with shadow region.

Keywords: *Thermal design, Micro satellites, Nano satellites, Sun-synchronous orbit*

NOMENCLATURE

a	albedo factor
A_p	projected area
A_{pmps}	projected area of MPS
A_{pbsdsp}	projected area of bottom side of DSP
A_{ptsdsp}	projected area of top side of DSP
A_{tsdsp}	a top surface area of DSP
A_{bsdsp}	a bottom surface area of DSP
A_{pmps1}	projected area of MPS consider the surface close to DSP
C_{mps}	specific Heat of MPS
C_{dsp}	specific Heat of DSP
F_{ns-e}	view factor from the earth pointing surface of MPS to the earth
F_{ps-e}	view factor from the surface parallel to the position vector of MPS to the earth
F_{ndsp-e}	view factor from the lower side DSP to the earth
F_{pdsp-e}	view factor from the surface parallel to the position vector of DSP to the earth.
$F_{fdps-mps}$	view factor from DSP to MPS
$F_{fmps-dsp}$	view factor from MPS to DSP
G_s	solar constant
l	length of each side of the satellite
m_{mps}	mass of MPS
m_{dsp}	mass of DSP
P_{gen1}	power generated by MPS
P_{gen2}	power generated by DSP
q_{IR}	earth Infrared Radiation
$\dot{Q}_{ds}$	solar direct
$\dot{Q}_{IR}$	heat input by Earth Infrared Radiation
$\dot{Q}_{com}$	heat generated from component
$\dot{Q}_{alb\text{-}fearth}$	heat input by Earth albedo
$\dot{Q}_{reflin\text{-}fdsp}$	reflected energy input from DSP to MPS
$\dot{Q}_{reflin\text{-}fdsp}$	reflected energy input from DSP to the MPS
$\dot{Q}_{radin\text{-}fmps}$	radiation absorbed by DSP from MPS
$\dot{Q}_{radin\text{-}fdsp}$	radiation absorbed by MPS from DSP
$\dot{Q}_{rad\text{-}fmps}$	radiation from MPS
$\dot{Q}_{rad\text{-}fdsp}$	radiation from DSP
$\dot{Q}_{shunt}$	heat produced due to shunt
$(\dot{Q}_{IR})_{fdsp}$	reflected energy by Earth IR radiation from DSP to MPS

[*] **Corresponding author:** Email: tilok_cuet@yahoo.com; Tel: 880-1866658473

$(\dot{Q}_{alb\text{-}fearth})_{fdsp}$	reflected energy by albedo of earth from DSP to MPS
$(\dot{Q}_{ds})_{fdsp}$	reflected energy by solar direct from DSP to MPS
$(\dot{Q}_{IR})_{fmps}$	reflected energy by Earth IR radiation from MPS to DSP
$(\dot{Q}_{alb\text{-}fearth})_{fmps}$	reflected energy by albedo of earth from MPS to DSP
$(\dot{Q}_{ds})_{fmps}$	reflected energy by solar direct from DSP to MPS
T_{dsp}	temperature of DSP
T_{mps}	temperature of MPS
T	time
t_c	thickness of DSP plate
θ_{za}	zenith angle between the normal vector of a surface and the vector to the sun
α_{mps}	solar absorptivity of MPS
α_{tsdsp}	solar absorptivity of bottom surface of DSP
α_{bsdsp}	solar absorptivity of bottom surface of DSP
ε_{mps}	emissivity of MPS
ε_{tsdsp}	emissivity of top surface of DSP
ε_{bsdsp}	emissivity of bottom surface of DSP
Σ	stefan-Boltzmann constant, 5.67×10^{-8} $(W/(m^2K^4))$
ρ_c	filling factor
n_c	solar cell efficiency

1. INTRODUCTION

Nano and Micro satellites are very popular now-a-days among different kinds of satellites that are sent into space. There are many reasons why it is getting wide acceptance in the field of space systems. First of all, it is cheaper in comparing with large and medium satellites and fabrication time can be abridged like one and half year after receiving the contract. New technologies can be implemented as an updating satellite system and its functioning. Moreover, it can be used for excellent teaching material to realize how its work in space for educational institutions. Applications of nano and micro satellites are not only limited in teaching tools for students, but also these kinds of satellites can be used for many business purposes such as observing disasters, flood or agricultural purposes. Micro and nano satellite do not have any propulsion system to shift from orbit of one local time of descending node to orbit of another local time of descending node with the help of the data handling system controlled by server from ground stations. There is a possibility to change the local time of descending node of micro and nano satellites due to oblateness of the Earth. It is important to have a good thermal design of micro and nano satellites for working it all components properly. In order to prepare micro and nano satellites within very short time, it is essential to establish guidelines to know some quantities and properties such as maximum power generation capacity of satellite during moving in different LTDN, surfaces optical properties, position of shunt either the main part of the satellite or DSP etc. The combination of optical properties of structures and components to keep the temperature within the design temperature range are clarified using one nodal, two nodal and multi-nodal analyses in case of satellite without DSP by Totani et al. [1]–[3]. But nano and micro satellites with DSP have some additional difficulties such as wide range of temperature variation due to larger amount of projected area to the sun and onset of shadow region on MPS due to DSP over satellite without DSP. This paper carries the two nodal analyses to obtain number of combinations of optical properties such as absorptivity and emissivity of micro and nano satellites with DSP in order to challenge those difficulties.

2. METHOD OF ANALYSIS

2.1 Projected Area of Satellite

Detail description about the projected area of Micro and Nano satellites of cube-shaped without DSP or body mounted solar panel has done for local of descending node from 6 to 12 at the same altitude of 500 km with respect to the Sun in winter solstice by Totani et al. [3]. Figures 1 and 2 show satellite with and without DSP respectively. The projected area of satellite with DSP is calculated and compared with satellite without DSP. Fig. 6 presents the comparison of projected area of satellite with and without DSP at the local time of descending node 10 and 500 km altitude with respect to the Sun in winter solstice without considering shadow region of Earth. Because in the case that satellite goes inside shadow region of Earth, there will be no projected area with respect to the Sun. Unit length is considered for the length of each side of the satellite. Projected area for satellite with DSP is the summation of the main part of the satellite, top and bottom side of DSP. The main purpose of using DSP in satellite is to increase the projected area to the Sun during moving in orbit for generating large amounts of power than satellite without DSP.

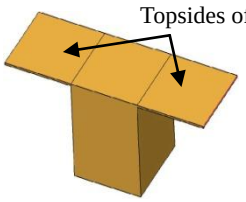

Fig. 1: Satellite with deployable solar panel.

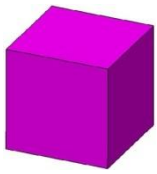

Fig. 2: Satellite without deployable solar panel.

2.2 Power Generation

It is very important to know that how much power can be generated by solar cells mounted on different surfaces. Maximum load can be installed inside the satellite depends on power generation capability by the solar cells. It is possible to determine the filling factor for satellite by this analysis that means how much surface will be covered of total surface area of satellite in order to satisfy power demand by load given inside of the satellite. Fig. 3 shows the schematic diagram considering the shadow and the sunshine region of satellite travelling on orbit. Depending on altitude and LTDN, satellite does or does not enter into the shadow region. For instance, at 500 km altitude a satellite does not enter into the shadow region of earth for local time of descending node 6 and 7 on sun-synchronous orbit in the winter solstice. “Considering satellite start moving from at the

entrance of shadow region ($t = t_s$) and satellite exit shadow region when $t = t_e$. It keeps moving in the sunshine region for a period, say $t = t_0$ and finally reach in initial position at $t = t_f$. The relation among all times from start to finish is given below.":

$$t_s < t_e < t_0 < t_f$$

Electricity is generated by solar cells only in the sunshine region. General equation is used for calculating power generation for one rotation in orbit by solar cell is shown below.

$$P_{gen} = \int_{t_s}^{t_f} \rho_c n_c G_s \left(A_p + aF_a l^2\right) dt \quad (1)$$

Different conditions can be considered for generating power, such as solar mounted on

a) All the surfaces covered with solar cells,

b) 6 surfaces and Topsides of DSP covered with solar cells,

c) 5 surfaces and Topsides of DSP that mean removing solar cells from the earth pointing surface and bottom surfaces etc.

In this paper, the result of case (c) is considered, because in practical case there is no solar cells on the Earth pointing surface due to separation system, telescope are mounted in this surface. Filling factor is equal 1 that means 5 surfaces and topsides of DSP covered with solar cells completely. Topsides of DSP do not receive any albedo from Earth, because those surfaces are in opposite direction to the surface always pointing to the Earth.

Table 1 shows the angle of the shadow region for local time of descending node from 6 to 12 at 500 km altitude. γ_1 represents angle at the entrance of shadow region and γ_2 at the exit of shadow region angle and finally γ indicates the angle of the shadow region for different LTDN which is equal the difference between γ_2 and γ_1. Table 2 shows information about the worst hot and worst cold case that is considered in this paper. Separate results were obtained from this analysis for both the worst hot and worst cold case.

In this case 8000 grid points are considered to calculate power generation by satellite with DSP.

Table 1 Angle of shadow region for 500 km altitude

LTDN	γ_1 (deg.)	γ_2 (deg.)	γ (deg.)
6	0	0	0
7	0	0	0
8	75.98	168.99	93.01
9	56.96	174.25	117.29
10	48.61	177.16	128.55
11	45.33	179.32	133.99
12	45.28	181.25	135.97

Table 2 Worst hot case and worst cold case

Parameter	Worst cold case	Worst hot case
Solar contact (W/m^2)	1309	1414
Earth infrared radiation (W/m^2)	189	261
Albedo factor	0.2	0.4
Initial temperature (°C)	10	25
Initial position for calculation	Entrance of eclipse	Exit of eclipse

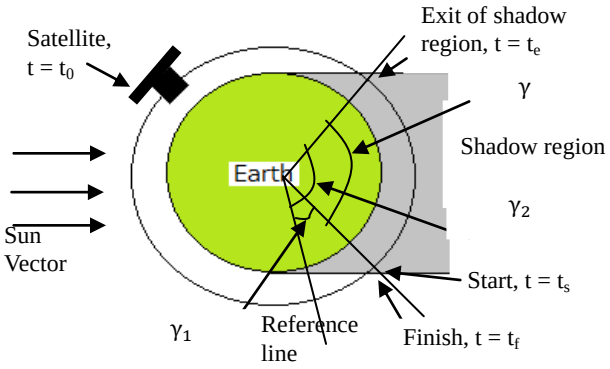

Fig. 3: Satellite moving in orbit.

2.3 Energy Equation

Table 3 and Table 4 show information about satellite model defined for this analysis. Fig. 4 shows input and output heat is considered for satellites with DSP model for analysis of optical properties. Basic schematic diagram and energy equations for satellite without DSP were presented by Totani et al. [4]. The basic difference in the schematic diagram of satellite with or without DSP is an additional heat exchange needed to consider such as reflection and radiation heat transfer from MPS to DSP and vice versa. Equations 2 and 3 for the main part of the satellite and DSP include radiation and reflection terms that are considered respectively. In the case of reflection, diffusive reflection is assumed. Equations for the main part of the satellite and DSP in this analysis are given separately.

Table 3 Shape, orbit, attitude, and setting method of solar panel of satellites analyzed in this paper.

Shape	Cube with deployable solar panel
Orbit	Sun-synchronous and circular orbit
Attitude	Earth-pointing
Altitude	500 km
Inclination	97.4 degrees
Setting method of solar panel	Body mounted and deployable solar panel.
Allowable temperature range of MPS.	0~40 degree Celsius
Allowable temperature range of DSP.	-145~ 65 degree Celsius

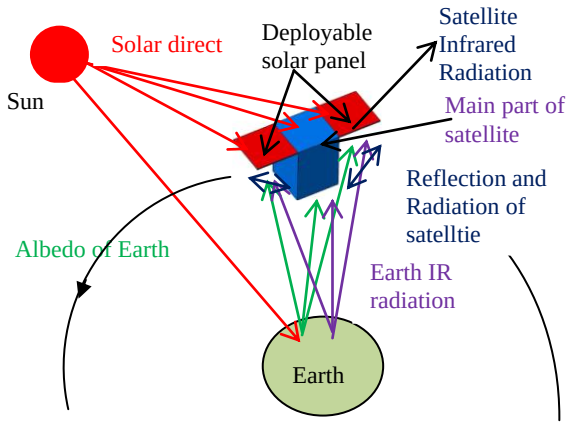

Fig. 4: Schematic of heat input and output from satellite.

Table 4 Size, mass, heat capacity of satellites

Mass of MPS, m_1 [kg]	50
Mass of DSP, m_2 [kg]	2
Size l^3 [cm^3]	50×50×50
Thickness of DSP plate, t [mm]	1.5
Heat capacity of MPS, m_1c [J/K]	36000
Heat capacity of DSP, m_2c [J/K]	1440

Equations for main part of satellite:

$$\dot{Q}_{ds} + \dot{Q}_{alb\text{-}fearth} + \dot{Q}_{IR} + \dot{Q}_{reflin\text{-}fdsp} + \dot{Q}_{radin\text{-}fdsp} + \dot{Q}_{com} - P_{mps} - \dot{Q}_{rad\text{-}fmps} + \dot{Q}_{shunt1} = m_{mps} C_{mps} \frac{dT_{mps}}{dt} \quad (2)$$

Where, $\dot{Q}_{ds} = \alpha_{mps}\, G_s\, A_{pmps}$

$\dot{Q}_{alb\text{-}fearth} = \alpha_{mps}\, G_s\, a\, (F_{n\,s-e}\, l^2 + 4\, F_{p\,s-e}\, l^2) \cos\theta_{za}$

$\dot{Q}_{IR} = \varepsilon_{mps}\, q_{IR}\, (F_{n\,s-e}\, l^2 + 4\, F_{p\,s-e}\, l^2)$

$\dot{Q}_{reflin\text{-}fdsp} = F_{fdsp-mps}\, (\varepsilon_{mps}\, \dot{Q}_{IR} + \alpha_{mps}\, \dot{Q}_{alb\text{-}fearth} + \alpha_{mps}\, \dot{Q}_{ds})_{fdsp}$ (considering diffusive reflection)

$(\dot{Q}_{IR})_{fdsp} = 2\,(1 - \varepsilon_{bsdsp})\, q_{IR}\, A_{bsdsp}\, F_{ndsp-e}$

$(\dot{Q}_{alb\text{-}fearth})_{fdsp} = 2\,(1 - \alpha_{bsdsp})\, G_s\, a\, A_{bsdsp}\, F_{ndsp-e} \cos\theta_{za}$

$(\dot{Q}_{ds})_{fdsp} = (1 - \alpha_{bsdsp}) G_s\, A_{pbsdsp}$

$\dot{Q}_{radin\text{-}fdsp} = 2\, \varepsilon_{mps}\, F_{fdsp-mps}\, \varepsilon_{bsdsp}\, A_{bsdsp}\, \sigma\, T_{dsp}^{\,4}$

$\dot{Q}_{rad\text{-}fmps} = \varepsilon_{mps}\, 6\, l^2 \sigma\, T_{mps}^{\,4}$

Equations for deployable solar panel of satellite:

$$\dot{Q}_{ds} + \dot{Q}_{alb\text{-}fearth} + \dot{Q}_{IR} + \dot{Q}_{reflin\text{-}fmps} + \dot{Q}_{radin\text{-}fmps} - P_{dsp} - \dot{Q}_{rad\text{-}fdsp} + \dot{Q}_{shunt2} = m_{dsp}\, C_{dsp} \frac{dT_{dsp}}{dt} \quad (3)$$

Where, $\dot{Q}_{ds} = \alpha_{tsdsp}\, G_s\, A_{ptsdsp} + \alpha_{bsdsp}\, G_s\, A_{pbsdsp}$

$\dot{Q}_{alb\text{-}fearth} = \alpha_{bsdsp}\, G_s\, a (2\, A_{bsdsp}\, F_{ndsp-e} + 6\, F_{pdsp-e}\, l\, t_c) \cos\theta_{za}$

$\dot{Q}_{IR} = \varepsilon_{bsdsp}\, q_{IR}\, (2\, A_{bsdsp}\, F_{ndsp-e} + 6\, F_{pdsp-e}\, l\, t_c)$

$\dot{Q}_{reflin\text{-}fmps} = F_{fmps-dsp}\, (\varepsilon_{bsdsp}\, \dot{Q}_{IR} + \alpha_{bsdsp}\, \dot{Q}_{alb\text{-}fearth} + \alpha_{bsdsp}\, \dot{Q}_{ds})_{fmps}$ (considering diffusive reflection)

$(\dot{Q}_{IR})_{fmps} = 2\,(1 - \varepsilon_{mps})\, q_{IR}\, F_{p\,s-e}\, l^2$

$(\dot{Q}_{alb\text{-}fearth})_{fmps} = 2\,(1 - \alpha_{mps})\, G_s\, a\, F_{p\,s-e}\, l^2 \cos\theta_{za}$

$(\dot{Q}_{ds})_{fmps} = (1 - \alpha_{mps})\, G_s\, A_{pmps1}$

$\dot{Q}_{radin\text{-}fmps} = 2\, \varepsilon_{bsdsp}\, F_{mps-fdps}\, \varepsilon_{mps}\, l^2 \sigma\, T_{mps}^{\,4}$

$\dot{Q}_{rad\text{-}fdsp} = 6\varepsilon_{bsdsp}\, l\, t_c \sigma T_{dsp}^{\,4} + (2\varepsilon_{tsdsp} A_{tsdsp} + 2\varepsilon_{bsdsp} A_{bsdsp}) \sigma T_{dsp}^{\,4}$

2.3 Optical Properties

In order to determine optical properties of satellite, two nodal analyses are considered that means one node in DSP and another one node in the main part of the satellite. Whole orbit is divided into 8000 grid points in order to calculate optical properties identifying entrance and exit of shadow region. It is difficult to fix the specific heat of the main part of the satellite and DSP. The specific heat is considered 720 J/(kg K) in such a way that temperature of components change easily. The value of specific heat corresponds to 80% of the specific heat of aluminum alloy A5052, 900 J/(kg K) [5]. Temperature is considered constant for whole main part of the satellite. Again two DSP are in the same temperature during obtaining optical properties from analyses. Fig. 5 shows a flow chart for two nodal analyses to obtain optical properties in this program. Maximum and minimum average power consumption is 100W and 40W respectively for this analysis. The interval for optical properties both absorptivity and emissivity of MPS of the satellite is 0.01 and the interval for optical properties both absorptivity and emissivity of DSP of the satellite is 0.1.

Table 5 Specifications of analyses program

Programming Language	Fortran 90
Compiler	g95
Variable type	Double precision

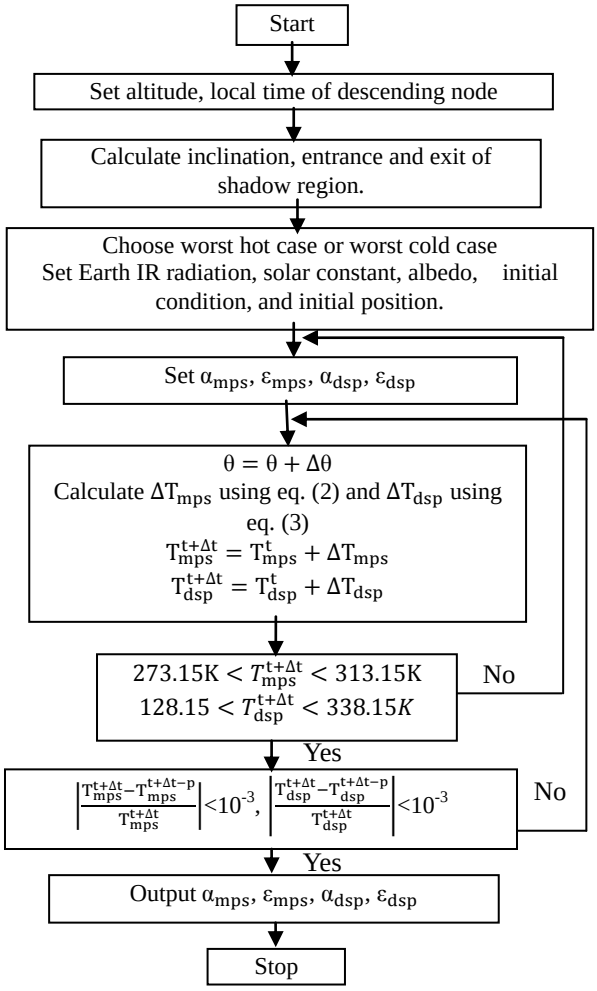

Fig. 5 Flow chart of optical properties calculation

3. RESULTS AND DISCUSSION

Fig. 6 shows the projected area of the satellite with and without DSP at LTDN 10. It presents that the projected area of satellite with DSP larger than satellite without DSP. It is obvious that the minimum projected area of satellite with DSP is as same as the satellite with body mounted solar panel. But the maximum projected area is large for long periods in the same orbit in the case that the satellite with DSP. Increasing the amount of projected area is important from the view point of generating large amount power for all components installed inside the satellite. The more generated power, the more components can be installed for obtaining information from satellites. In this case, the projected area of the satellite at LTDN 10 is compared to show the advantage from DSP. Fig. 7 shows average power that can be generated on orbit. From the analysis, it is observed that power generation of satellite increase with the increase of the number of LTDN. But power generation reduced at LTDN 8 as shown in Fig. 7, because it entered into the shadow region at

LTDN 8 and 500 km altitude. Again power generation of satellite started increasing due to increase in the projected area of satellite with DSP from LTDN 6 to 12.

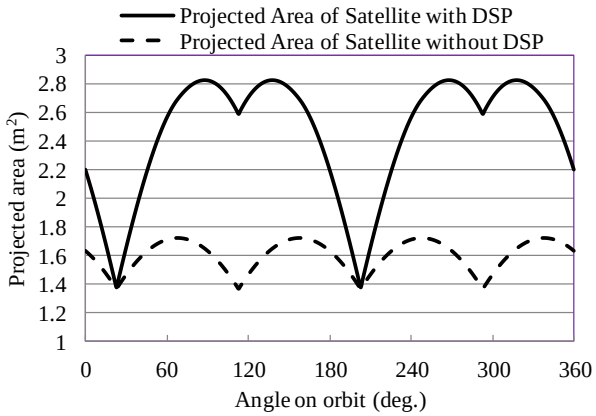

Fig. 6: Comparison of projected area of satellite with and without deployable solar panel at LTDN 10.

It is possible to obtain maximum power generation at LTDN 11 considering the angle of shadow region. The projected area of satellite with DSP at LTDN 12 increased, but at same time angle of shadow region also increased. From Table 6 show peak power that was obtained from analysis at LTDN 11 and 12 with the angle of shadow region. It is observed that peak power for LTDN 12 higher than LTDN 11 and the angle of shadow region for LTDN 11, and 12 are 133.99 and 135.97 degree respectively at 500 km altitude. Therefore, the maximum amount of average power generation could not be obtained at LTDN 12. Figures 8 and 9 show generated power of satellite at each point in orbit at LTDN 7 and 8 respectively. It is clear the reason why power generation dropped in case of LTDN 8. It can be seen from Fig. 8 that there is a continuous power generation of satellite with DSP at LTDN 7, because there was no shadow region of Earth. The satellite passes both shadow and sunshine region in the case of LTDN 8 as shown in Fig. 9. Similarly, from LTDN 9 to12, there is no power generation in the shadow region. Thus, it can be concluded that in order to generate maximum power, the satellite must be placed in the higher number of LTDN such as 10, 11, and 12.

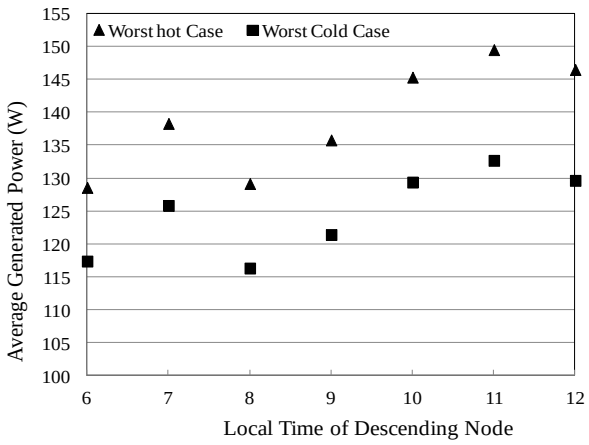

Fig. 7: Average generated power in different LTDN.

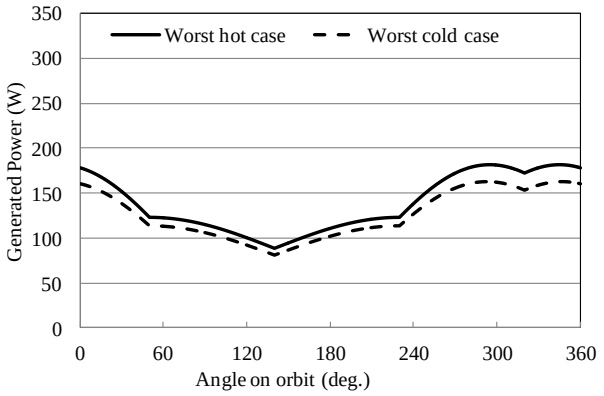

Fig. 8: Power generated by solar cells at LTDN 7.

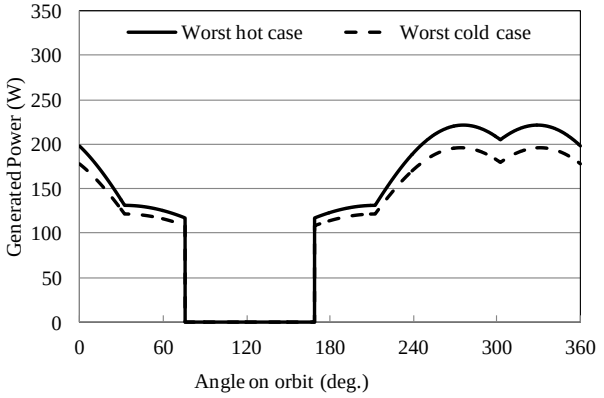

Fig. 9: Power generated by solar cells at LTDN 8.

Table 6 Peak power generation at LTDN 11 and 12

LTDN	Peak Power (W)		Angle of shadow region (deg.)
	Worst hot case	Worst cold case	
11	328.39	287.06	133.99
12	338.56	295.52	135.97

Figures 10, 11 show the combinations of optical properties at LTDN 8, and 11 respectively. The shunt is placed on DSP arbitrarily in this analysis and numbers of combinations are obtained at different LTDN at the altitude of 500 km. The number of combinations is decreasing with increase of LTDN. The reason why it happened that the projected area of the satellite with DSP are increasing with increase of the number of LTDN and there was no shadow region for LTDN 6 and 7 at 500 km altitude, but satellites enter into the shadow region from LTDN 8. At that situation, the numbers of combinations of optical properties were decreased significantly. It is the result of difficulties to satisfy the allowable temperature range 0 to 40 degrees Celsius for MPS including all components and -145 to 65 degree Celsius for DSP. The numbers of combinations of optical properties were maximum for the LTDN of 6 and 7 that means when there is no shadow region. Later with the increase of LTDN and angle of shadow region, number of combinations of optical properties reduced. These combinations of optical properties of the main part of satellite are not independent itself, but it also depends on the combination of optical properties of DSP because there is a heat transfer by reflection and radiation.

Conduction heat transfer between MPS and DSP is restricted by using adiabatic spacers so that the variation of temperature of the satellite with DSP could be minimized. The number of combinations of optical properties could be increased if the interval of optical properties of DSP of the satellite decreased from 0.1 to less for instance 0.01. Fig. 12 shows the temperature history corresponding two specific combinations of optical properties where one satisfies an allowable temperature range and other does not satisfy the allowable temperature range of satellite with DSP. Many combinations of optical properties corresponding to different coatings can be found in Gilmore's book in Appendix A [6].

Table 7 Relation of LTDN with Combination of Optical properties

LTDN	Number of Combination of optical properties in main part of satellite
6	1147
7	1257
8	412
9	169
10	95
11	57
12	42

In case of absorptivity 0.66 and emissivity 0.48, temperature history of satellite does not exceed the range of 0 to 40 degree Celsius that combinations of optical properties were obtained from two nodal analysis of satellite with DSP. On the other hand, temperature history of satellite of MPS drops below the lower limit of allowable temperature range in case of absorptivity 0.66 and emissivity 0.61. Although the temperature of satellite in the worst hot case keeps inside temperature range, but the temperature goes below 0 degree Celsius in case of the worst cold case. It is very important to choose a combination of suitable optical properties of satellite in order to keep the temperature of satellites in allowable temperature range.

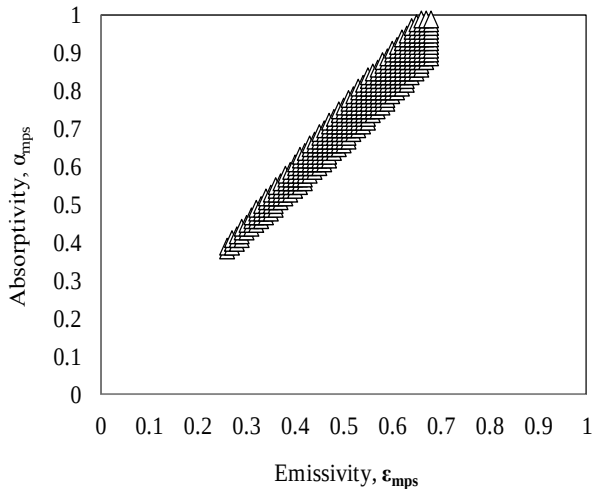

Fig. 10: Combinations of optical properties at LTDN 8.

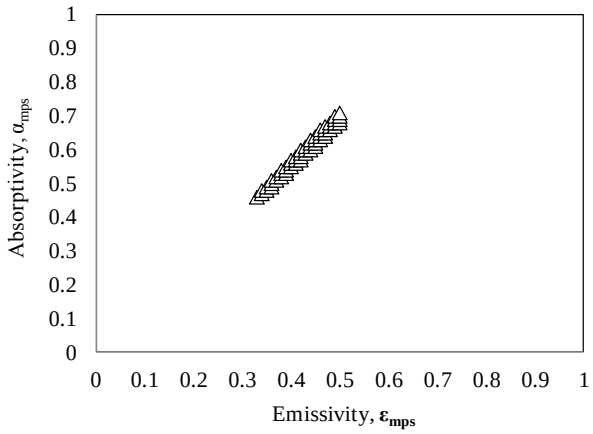

Fig. 11: Combinations of optical properties at LTDN 11.

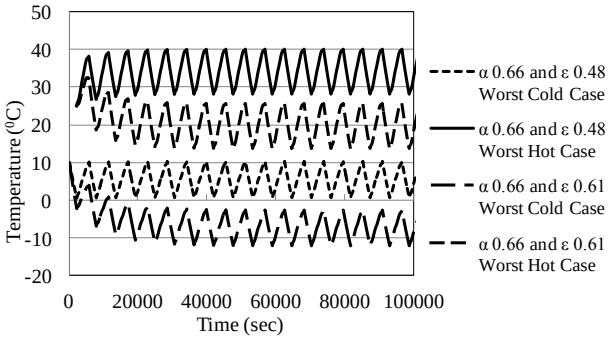

Fig. 12: Temperature history of main part of satellite at LTDN 11 for different combination of optical properties.

4. CONCLUSIONS

The projected area of satellite with and without DSP was compared at LTDN 10 in this paper. Average generated power of satellite with DSP was shown from LTDN 6 to 12 considering a satellite each side length of 50 cm in order to explain the maximum power that a satellite can provide assuming surfaces covered with solar cells completely. Highest average generated power 149.47 W and 132.65 W was obtained for LTDN 11 in the worst hot case and worst cold case respectively among all LTDN from 6 to 12. Power generation for different LTDN has a good image for future satellite load installment. At last, Maximum number of combinations of optical properties was obtained at LTDN 6 and 7 that means when there was no shadow region of Earth. Two nodal analyses were considered for determining combinations of optical properties of satellite with DSP where the main part of the satellite is one node and another node is DSP and the shunt is mounted on MPS.

5. ACKNOWLEDGMENTS

This research is granted by the Japan Society for the promotion of Science (JSPS) through the "Funding Program for World-Leading innovative R&D on Science and Technology (First Program)," initiated by the council for Science and Technology Policy (CSTP).

REFERENCES

[1] T. Totani, H. Ogawa, R. Inoue, T. K. Das, M. Wakita, and H. Nagata, "Thermal design procedure for micro- and nanosatellites pointing to Earth," Journal of Thermophysics and Heat Transfer, Vol. 28, No.3, pp. 524–533, 2014.

[2] T. Totani, H. Ogawa, R. Inoue, T. K. Das, M. Wakita, and H. Nagata, "New Procedure for Thermal Design of Micro- and Nano- Satellites Pointing to Earth," Transactions of the Japan Society for Aeronautical and Space Sciences, Aerospace Technology Japan, Vol. 12, No. 29, pp. 11−20, 2014.

[3] R. Inoue, T. Totani, H. Ogawa, M. Wakita, H. Nagata, "Thermal analyses and guideline of Nano and Micro satellites on Sun-synchronous orbits" 4th Nano Satellite Symposium, October 10v13, 2012, Nagoya, Japan.

[4] T. Totani, H. Ogawa, R. Inoue, M. Wakita, H. Nagata, "One Nodal Thermal analysis for Nano and Micro satellites on Sun-synchronous orbits" Trans. JSASS Aerospace Tech. Japan, Vol. 11, pp. 71v78, 2013.

[5] Japan Aluminum Association, Characteristics Data base of Aluminum Materials [online database] Available: http://metal.matdb.jp/JAA-DB/ (cited 4 March2013).

[6] D. G. Gilmore, Spacecraft Thermal control Handbook, 2nd ed., Vol. 1, the aerospace Press, EI Segundo, 2002, Appendix A.